

Where do polymer adhesives fail?

D. GERSAPPE and M. O. ROBBINS

*Department of Physics and Astronomy, The Johns Hopkins University
Baltimore, MD 21218, USA*

(received 26 February 1999; accepted in final form 24 August 1999)

PACS. 36.20Ey – Conformation (statistics and dynamics).

PACS. 61.41+e – Polymers, elastomers, and plastics.

PACS. 68.35Gy – Mechanical and acoustical properties; adhesion.

Abstract. – We use molecular-dynamics simulations of a polymer film confined between two walls to isolate the factors that control where an adhesive bond breaks. Failure occurs either at the wall/film interface (adhesive failure) or within the film (cohesive failure). Most theories relate the location of failure to equilibrium interfacial free energies. However, we find that the location of failure coincides with the region of lowest initial yield stress and cannot be predicted from equilibrium interfacial free energies.

The strength of an adhesive bond is intimately related to the details of where and how the bond ruptures. Although the rupture process generally occurs very far from equilibrium, theories have assumed that both the location of failure and the work required to break a unit area, G , are controlled by the increase in equilibrium interfacial free energy $\Delta\gamma$ at the surfaces created during rupture [1, 2]. In particular, failure is assumed to occur at the interface where $\Delta\gamma$ is smallest, and G is assumed to be proportional to $\Delta\gamma$.

A growing number of experimental and theoretical results is at odds with these predictions based on equilibrium free energies. Experiments on viscoelastic adhesives [3] found that values of G could not be correlated to the surface free energy. Simulations [4] and experiments [5] on glassy polymer films indicate that failure does not occur at the interface with the lowest $\Delta\gamma$. Studies of biological ligand/receptor bonds indicate that strength correlates with enthalpies rather than free energies [6]. This body of work raises very broad and general questions about whether interfacial free energy or some other property controls the strength and failure mode of adhesive bonds. Resolving these questions will have far-reaching implications, since adhesive properties are critical to the functioning of systems as diverse as composite structural materials and living organisms.

In this letter, we use molecular-dynamics simulations to isolate the factors that control the location of failure in polymeric adhesives. Failure can occur either at the substrate/adhesive interface (adhesive failure) or in the center of the adhesive (cohesive failure). Cohesive failure leads to more dissipation and a stronger bond. The condition that failure should occur where $\Delta\gamma$ is smallest is equivalent to saying that cohesive failure should occur only when the adhesive

completely wets the substrate. However, we show that the transition from adhesive to cohesive failure does not correlate with the onset of complete wetting. Instead, the location of failure is determined by the local yield stress in early stages of rupture. We also find that in our system the location of failure is independent of both temperature and polymer length, and thus that interfacial entropies do not influence the mode of failure.

In our simulations an adhesive film is confined between two rigid, solid walls. The film consists of linear polymers each containing L monomers. Except where noted, $L = 16$. Monomers of mass m , separated by a distance r , interact through a truncated Lennard-Jones (LJ) potential of the form [7]

$$V(r) = 4\epsilon[(\sigma/r)^{12} - (\sigma/r)^6], \quad (1)$$

for $r < r^c = 2.2\sigma$. Here ϵ and σ are the characteristic energy and length scales, and the potential is zero for $r > r^c$. Adjacent monomers along the chain are coupled by an additional potential:

$$V^{\text{CH}}(r) = -(1/2)kR_o^2 \ln[1 - (r/R_o)^2], \quad \text{for } r < R_o, \quad (2)$$

where $R_o = 1.5\sigma$ and $k = 30\epsilon/\sigma^2$. Previous studies have shown that this potential prevents chain breaking and yields realistic dynamics for polymer melts [8].

Each wall consists of atoms forming two (111) planes of an fcc lattice, with the atoms of the walls connected to the lattice sites by stiff springs. The wall density was set to twice the monomer density to reduce epitaxial effects [9]. A LJ potential with modified parameters ϵ_{wa} , $\sigma_{\text{wa}} = \sigma$, and $r_{\text{wa}}^c = 2.2\sigma_{\text{wa}}$ was used to model the interactions between the adhesive monomers and the wall atoms. The value of the wall-adhesive coupling, ϵ_{wa} , was varied from 0.5 to 3.0 ϵ . Increasing ϵ_{wa} causes the adhesive to completely wet the walls.

The temperature T was kept constant by coupling the wall atoms to a heat bath [8]. Periodic boundary conditions were applied within the plane of the walls to eliminate edge effects. The equations of motion were integrated using a fifth-order predictor-corrector algorithm with a time step of $\Delta t = 0.005\tau$, where $\tau = (m\sigma^2/\epsilon)^{1/2}$. In the results presented below, the adhesive consisted of 1024 monomers and each wall had 200 monomers. Runs with half as many or twice as many monomers gave equivalent results.

Theories based on equilibrium free energies predict that the transition between adhesive and cohesive failure occurs at the point where the adhesive begins to completely wet the substrate. This happens when the spreading power S decreases to zero, where $S \equiv \gamma_{\text{av}} + \gamma_{\text{wa}} - \gamma_{\text{wv}}$, and γ_{av} , γ_{wa} , and γ_{wv} are the adhesive-vapor, wall-adhesive and wall-vapor interfacial tensions, respectively. We calculated S using the Kirkwood-Buff formulation [10] which equates the interfacial tension to the integral, through the interface, of the difference between the normal and tangential components of the pressure-stress tensor. This approach has been successfully used to calculate contact angles between liquids and the solid walls used here [11]. We obtained S from a single simulation of a polymer film in contact with only one wall.

In fig. 1, we plot S as a function of the coupling between adhesive and wall atoms, ϵ_{wa} , at two temperatures. At $T = 1.1\epsilon/k_B$ the polymer is in the fluid phase while at $T = 0.3\epsilon/k_B$ it is deep within the glassy state [4]. From the plot, the equilibrium prediction for the transition between adhesive and cohesive failure is at $\epsilon_{\text{wa}} = 2.8\epsilon$ for $T = 0.3\epsilon/k_B$ and $\epsilon_{\text{wa}} = 1.6\epsilon$ for $T = 1.1\epsilon/k_B$.

To determine the actual transition between adhesive and cohesive failure, we first confined the polymer film between two walls and allowed it to equilibrate at zero pressure. We then separated the walls with a uniform velocity v and monitored the particle positions and forces in the system. All the results presented below were for a velocity of $v = 0.03\sigma/\tau$, but similar results were obtained for $v = 0.003\sigma/\tau$.

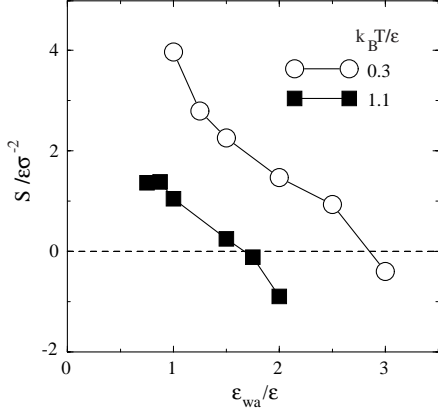


Fig. 1

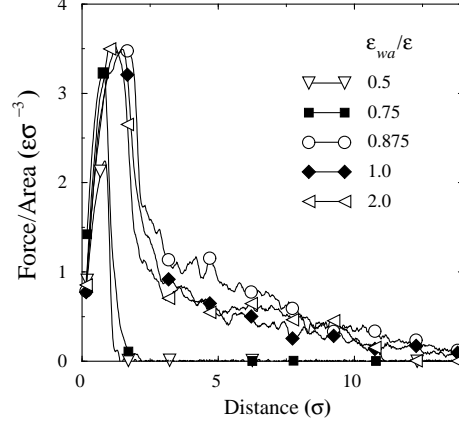


Fig. 2

Fig. 1. – The spreading power S for polymer films with a chain length of $L = 16$ at the two indicated temperatures, $k_B T / \epsilon = 0.3$ and 1.1 . The wetting transition ($S = 0$) is located at $\epsilon_{wa} / \epsilon = 2.8$ and 1.6 for $k_B T / \epsilon = 0.3$ and 1.1 , respectively. The size of the error bars is comparable to the symbol sizes used in the figure.

Fig. 2. – Force *vs.* wall displacement for polymer films being pulled apart with velocity $v = 0.03\sigma/\tau$ at the indicated values of ϵ_{wa} / ϵ . The transition between adhesive and cohesive failure is at $\epsilon_{wa} = 0.875\epsilon$.

In fig. 2 we plot the external force on the system as a function of wall displacement for different values of ϵ_{wa} at $T = 0.3\epsilon/k_B$. From the plot we see that the maximum in the force-displacement curve rises with increasing ϵ_{wa} until we reach a transition at $\epsilon_{wa}^t = 0.875\epsilon$. At this point we find that the location of failure shifts from the wall interface to the center of the film. Note that this transition occurs far below the equilibrium prediction (0.875 *vs.* 2.8ϵ). For $\epsilon_{wa} > 0.875\epsilon$, the maximum force no longer increases, and the force-displacement curves for all ϵ_{wa} nearly coincide.

The maximum in the force-displacement curve corresponds to the first yield event in the system. At $\epsilon_{wa} = 0.5\epsilon$ the bond between the adhesive and the wall is weak. The maximum in the force-displacement curve corresponds to the yield stress at the wall interface. As we increase ϵ_{wa} , the interfacial yield stress at the wall increases roughly linearly with ϵ_{wa} . For $\epsilon_{wa} > 0.875\epsilon$ the yield stress at the wall interface is larger than the yield stress of the film. Since failure now occurs within the film, ϵ_{wa} has no effect on the yield stress and the peak in the force-displacement curves saturates. This saturated value equals the interfacial yield stress at the transition from adhesive to cohesive failure at $\epsilon_{wa} = 0.875\epsilon$. Thus our results show that failure occurs where the initial yield stress is smallest.

A signature of the transition between adhesive and cohesive failure is the appearance of a long tail in the force-displacement curve. This implies that the work to failure (given by the integral of the force-displacement curve) is much larger for cohesive failure than adhesive failure. This can be clearly seen in fig. 3 where we plot the work to failure as a function of ϵ_{wa} . At both $k_B T / \epsilon = 0.3$ and 1.1 , the transition to cohesive failure occurs at $\epsilon_{wa}^t = 0.875\epsilon$. The work increases with ϵ_{wa} below the transition and is constant at larger ϵ_{wa} . It is surprising that the transition between adhesive and cohesive failure occurs at the same value of ϵ_{wa} in the fluid and glassy states. This is in contrast to the equilibrium predictions where increasing the temperature shifts the wetting transition, and hence the predicted transition between adhesive and cohesive failure, from $\epsilon_{wa} / \epsilon = 2.8$ to 1.6 .

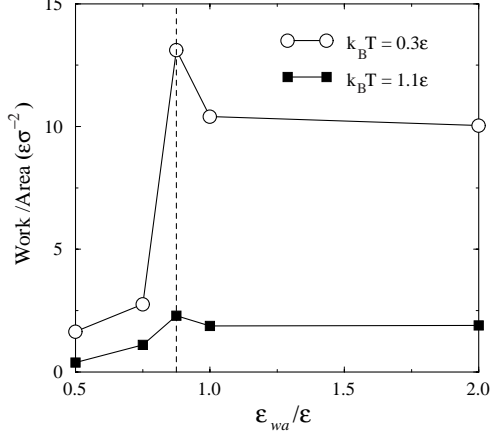


Fig. 3

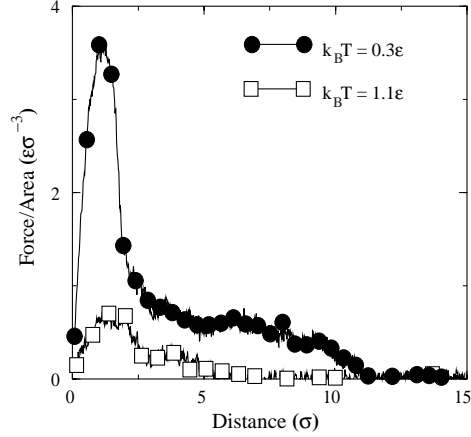


Fig. 4

Fig. 3. – Work to failure for the two indicated temperatures $k_B T/\epsilon = 0.3$ and 1.1 as a function of ϵ_{wa} . The dashed line indicates the transition between adhesive (left) and cohesive failure (right).

Fig. 4. – Force *vs.* wall displacement for $k_B T/\epsilon = 0.3$ and 1.1 at $\epsilon_{wa} = 2\epsilon$ and $v = 0.03\sigma/\tau$.

Although the value of ϵ_{wa}^t is independent of temperature, the magnitude of the increase in work at ϵ_{wa}^t is bigger in the glassy state (fig. 3). Force-displacement curves for $\epsilon_{wa} = 2\epsilon$ at $k_B T/\epsilon = 0.3$ and 1.1 are compared in fig. 4. As in experiments [12], the yield stress decreases with increasing temperature. In our model, the interfacial and cohesive yield stress drop at the same rate, so that there is no change in ϵ_{wa}^t . This may be because the wall/monomer and monomer/monomer interactions have the same simple LJ form. More realistic potentials could lead to different temperature dependence at the interface than in the bulk [13], causing a shift in the mode of failure with temperature like that seen in some experiments [14, 15]. The increase in work at low temperature also reflects a lengthening of the tail in the force-displacement curve (fig. 4) due to different mechanisms of rupture in fluid and glassy states [4, 16].

The lack of temperature dependence in ϵ_{wa}^t for our systems indicates that entropy plays little role in controlling the transition between adhesive and cohesive failure. Another way of varying the entropy is by changing the chain length, since increasing the chain length increases the conformational entropy. In fig. 5 we plot the work to failure for two polymer films, one with $L = 16$ and the other with $L = 2$. Both films are at a temperature of $T = 0.3\epsilon$. Once again, we see that the transition between adhesive and cohesive failure occurs at the same value $\epsilon_{wa}^t = 0.875\epsilon$. However, the total work to failure does depend on the chain length, with longer chains providing a stronger adhesive joint at large ϵ_{wa} . This increase is almost entirely due to changes in the tail of the force-displacement curve. The yield stress is nearly independent of chain length, even when the chain length is increased far beyond the entanglement length [17].

The equilibrium prediction for ϵ_{wa}^t/ϵ would shift from 2.8 to 2.1 as L changed from 16 to 2 . To understand the sizable discrepancy between simulation results and free-energy predictions we must follow the microscopic rearrangements that occur during the rupture process. As we start moving the walls apart, the film deforms elastically. This region is the linear region in the force-displacement curves (see fig. 2). In this elastic regime, the relative motions of atoms are still small compared to the interatomic spacing. The stress that is built up in the system is a result of nearly affine stretching of intermolecular bonds, without changing the chain

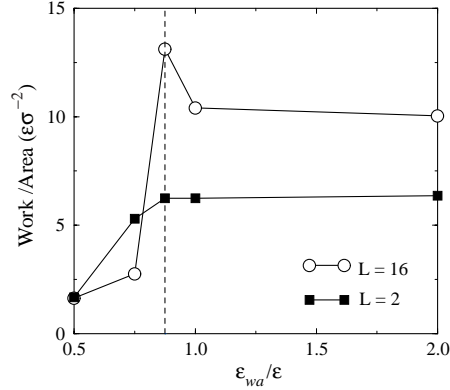


Fig. 5. – Work to failure for two chain lengths $L = 2$ and 16 as a function of ϵ_{wa} . The temperature was fixed at $T = 0.3\epsilon/k_B$ in both cases. The dashed line indicates the transition between adhesive (left) and cohesive (right) failure.

conformations. The first yield event, corresponding to the maximum in the force-displacement curve, occurs when some of the intermolecular bonds break. Their strength is determined by the LJ interaction potential. Until the bonds break, the atoms only respond to their local environment and do not feel the effect of chain connectivity.

After the first yield event, cavities start to form within the film. The location of the initial cavity is critical to the type of failure in the film. This is because stress is concentrated at the edge of the cavity making it the most likely site for subsequent failure. At low values of ϵ_{wa} the bonds between the adhesive and the wall are weak and so the initial cavity nucleates at the wall-adhesive interface. Once this happens, the film simply peels away from the wall, resulting in adhesive failure. When ϵ_{wa} increases past a critical value, the first cavity forms within the polymer film and the mode of failure is then cohesive in nature. Further increases in ϵ_{wa} have no effect, since yield has shifted to the interior of the film. Therefore, the location of failure in the adhesive is controlled by the weakest link in the system, or the location of the first yield event. At lower wall-adhesive coupling this takes place at the wall, while at higher ϵ_{wa} yield takes place in the interior of the film.

We note that in our present system the applied load is purely tensile in nature. As a result of the periodic boundary conditions, the internal stress can only be relieved by cavitation. We have also studied finite films to determine how edges change the failure mechanism. Although edges introduce shear stresses and may alter the way molecules rearrange during yield events, the basic conclusions remain the same. We still find that the location of failure does not correlate with free-energy differences and that changes in temperature and chain length have no noticeable effect on ϵ_{wa}^t .

Our results have important consequences. The obvious one is that any argument based on the free energy of the system cannot predict the transition between adhesive and cohesive failure. This conclusion is consistent with recent experiments that show cohesive failure even when the substrates have been altered so that the epoxy adhesive is non-wetting [5]. We find that the location of failure occurs where the local yield stress is smallest. This initial yield stress is controlled by intermolecular binding energies and not the conformational entropy of the chain molecules. This is an unusual phenomenon for polymeric systems where conformational entropy is often the dominant factor. However, experiments on biological ligand/receptor bonds [6] also indicate that entropy is less important than enthalpy in controlling rupture.

Cohesive failure requires much more work than adhesive failure, and thus produces a much stronger bond. One reaches the paradoxical conclusion that in some cases it may be possible to make a stronger joint by weakening the bonds between adhesive molecules. In particular, the adhesive-adhesive bonds must be slightly weaker than the wall-adhesive bonds in order to gain the increased dissipation associated with cohesive failure.

Many practical adhesives increase dissipation by using entangled or crosslinked polymers. Work in progress shows that this does not change the location of the initial cavities [17, 18]. However, crosslinks and entanglements limit the growth of cavities during cohesive failure. Strain hardening in the initial failure zone causes new cavities in adjacent regions of the adhesive. This leads to tremendous increases in the dissipation as the entire volume of the adhesive is transformed into a craze. Failure may eventually shift to the interface after the entire adhesive has strain hardened, unless chain scission occurs or crosslinks break. This type of process is clearly difficult to describe in terms of equilibrium thermodynamic quantities like the free energy.

Several non-equilibrium factors that are not included in our simulations may also influence the location of failure. One is the presence of pre-existing stress in the bond due, for example, to thermal contraction [19]. Another is the distribution of stress near the crack tip due to the bulk viscoelastic response of the adhesive and bonded materials. Such issues remain a challenge for future simulations.

We would like to thank Dr. A. BALJON for useful discussions. Financial support from National Science Foundation grant DMR-9634131 is gratefully acknowledged.

REFERENCES

- [1] LEE L.-H. (Editor), *Fundamentals of Adhesion* (Plenum Press, New York) 1991; CHAUDHURY M. K., *Mat. Sci. Engin. R*, **16** (1996) 97.
- [2] GENT A. N. and SCHULTZ J., *J. Adhesion*, **3** (1972) 281.
- [3] NEWBY B. Z., CHAUDHURY M. K. and BROWN H. R., *Science*, **269** (1995) 1407.
- [4] BALJON A. R. C. and ROBBINS M. O., *Science*, **271** (1996) 482.
- [5] KENT M., private communication.
- [6] GRÜBMULLER H., HEYMANN B. and TAVAN P., *Science*, **271** (1996) 997.
- [7] ALLEN M. P. and TILDESLEY D. J., *Computer Simulation of Liquids* (Clarendon, Oxford) 1987.
- [8] KREMER K. and GREST G. S., *J. Chem. Phys.*, **92** (1990) 5057.
- [9] THOMPSON P. A. and ROBBINS M. O., *Phys. Rev. A*, **41** (1991) 6830.
- [10] KIRKWOOD J. G. and BUFF F. P., *J. Chem. Phys.*, **19** (1949) 539.
- [11] THOMPSON P. A., BRINCKERHOFF W. B. and ROBBINS M. O., *J. Adhesion*, **7** (1993) 535.
- [12] GENT A. N. and LINDLEY P. B., *Proc. R. Soc. London, Ser. A*, **249** (1958) 195.
- [13] For example the atomic spacings and arrangements within the region of the polymer that we model with a single spherical monomer will change with T . This will affect bonding to the wall and other monomers in different ways.
- [14] GENT A. N. and PETRICH R. P., *Proc. R. Soc. London, Ser. A*, **310** (1969) 433.
- [15] The distribution of stress in a fracture experiment will also change with T and may alter the mode of failure.
- [16] MOTT P. H., ARGON A. S. and SUTER U. W., *Philos. Mag. A.*, **68** (1993) 537.
- [17] ROBBINS M. O., BALJON A. R. C. and GERSAPPE D., in *Proceedings of the 22nd Annual Meeting of the Adhesion Society*, edited by D. R. SPETH, Vol. **376** (1999); BALJON A. R. C. and ROBBINS M. O., unpublished results.
- [18] BARSKY S. and ROBBINS M. O., unpublished results.
- [19] AKISANYA A. R. and FLECK N. A., *Int. J. Fracture*, **55** (1992) 29; **58** (1992) 93.